Plant Reprod (2013) 26:125–137
DOI 10.1007/s00497-013-0215-x

ORIGINAL ARTICLE

Transgenic manipulation of plant embryo sacs tracked through cell-type-specific fluorescent markers: cell labeling, cell ablation, and adventitious embryos

Shai J. Lawit · Mark A. Chamberlin · April Agee · Eric S. Caswell · Marc C. Albertsen

Received: 30 January 2013 / Accepted: 13 March 2013 / Published online: 29 March 2013

Abstract Expression datasets relating to the *Arabidopsis* female gametophyte have enabled the creation of a tool set which allows simultaneous visual tracking of each specific cell type (egg, synergids, central cell, and antipodals). This cell-specific, fluorescent labeling tool-set functions from gametophyte cellularization through fertilization and early embryo development. Using this system, cell fates were tracked within *Arabidopsis* ovules following molecular manipulations, such as the ablation of the egg and/or synergids. Upon egg cell ablation, it was observed that a synergid can switch its developmental fate to become egg/embryo-like upon loss of the native egg. Also, manipulated was the fate of the somatic ovular cells, which can become egg- and embryo-like, reminiscent of adventitious embryony. These advances represent initial steps toward engineering synthetic apomixis resulting in seed derived wholly from the maternal plant. The end goal of applied apomixis research, fixing important agronomic traits such as hybrid vigor, would be a key benefit to agricultural productivity.

Keywords Egg cell ablation · Adventitious embryony · Apomixis · Embryo sac · Female gametophyte · Synergid ablation

Communicated by Anna Maria G Koltunow.

Electronic supplementary material The online version of this article (doi:10.1007/s00497-013-0215-x) contains supplementary material, which is available to authorized users.

S. J. Lawit (✉) · M. A. Chamberlin · A. Agee · E. S. Caswell · M. C. Albertsen
Agricultural Biotechnology, DuPont Pioneer, 7300 NW 62nd Ave, PO Box 1004, Johnston, IA 50131-1004, USA
e-mail: shai.lawit@pioneer.com

Introduction

The two-staged life cycle of plants alternates between a multicellular diploid organism, the sporophyte, and a multicellular haploid organism, the gametophyte. In angiosperms, the male and female gametophytes are surrounded by floral sexual organs, the anther and pistil, respectively. The female germ line develops from the nucellus. In female sexual development, a meiotic division (recently reviewed by Crismani et al. 2013) produces four megaspores, one of which develops into the functional megaspore via a cytokinin spatial cue (Cheng et al. 2013). In the common and well-characterized polygonum-type development, the functional megaspore undergoes three mitotic divisions forgoing intermediate cellularization steps and forming the syncytial female gametophyte containing eight haploid nuclei. This is the case in many species, including the model plant *Arabidopsis* as well as maize, soybean, and other agronomically important crops (reviewed by Yadegari and Drews 2004). Nuclear migration and auxin gradients lead to cell specification (Pagnussat et al. 2009) followed by cellularization. This process results in formation of a mature female gametophyte with seven cells: three antipodal cells, two synergid cells, one egg cell, and one central cell containing two polar nuclei that fuse prior to or during fertilization (reviewed by Berger and Twell 2011; Sprunck and Gross-Hardt 2011; Sundaresan and Alandete-Saez 2010). The synergid cells (reviewed by Li et al. 2009) secrete pollen tube attractants (Higashiyama et al. 2001; Marton et al. 2005; Sprunck et al. 2012) and serve as the first point of contact with pollen tubes that will ultimately deliver two sperm cells. In the process of fertilization, one of the two synergid cells is penetrated by the pollen tube resulting in synergid cell death. One sperm cell fuses with the egg cell and the other

fuses with the polar nuclei (2n) of the central cell (reviewed by Berger et al. 2008). The fertilized 2n egg cell (zygote) and 3n central cell develop into the embryo and endosperm, respectively (reviewed by Ingram 2010).

Female gametophyte structures are embedded within several layers of female ovular tissues (Fig. 1a) and are therefore difficult to access and visualize with traditional methods. Even in *Arabidopsis*, which has relatively transparent integuments, the embryo sac is surrounded by five cell layers which make observation difficult without chemical fixation and protracted clearing of whole ovules. This is one reason why relatively few studies have dealt with changes of cell fate within ovules (Gross-Hardt et al. 2007; Matias-Hernandez et al. 2010; Olmedo-Monfil et al. 2010; Pagnussat et al. 2007). To date, only individual cell identity within the embryo sac has been facilitated through GUS marker lines (Gross-Hardt et al. 2007; Vielle-Calzada et al. 2000; Yang et al. 2005) that offer a clear visualization of expression through staining patterns, or alternative approaches with individual fluorescent markers (Völz et al. 2012). Several studies have used gametophyte mutants to concentrate on elucidating gene expression patterns (Johnston et al. 2007; Ohnishi et al. 2011; Sánchez-León et al. 2012; Steffen et al. 2007; Wuest et al. 2010; Yu et al. 2005), allowing for identification of promoters for genes that are specifically expressed in the cells of the embryo sac. These specific expression patterns are useful for fluorescent visualization of individual live cells as described herein.

We discuss the development of a multi-color fluorescent reporter system designed to specifically and simultaneously visualize the four individual cell types of the megagametophyte (Fig. 1b, c), facilitating visual tracking of each cell type from embryo sac cellularization through fertilization and early embryo development. This system and variants thereof were utilized to investigate manipulations of the embryo sac and ovular cells in transgenic *Arabidopsis*. We produced stable transgenic lines with ablated synergids or egg cells while still maintaining surrounding cell health and development. The specific prevention of sexual embryos is a significant step toward synthetic apomixis, clonal reproduction through seed. The next more challenging step in producing clonal embryo material was the induction of maternally derived adventitious embryos, which were created here at a low frequency and tracked with the fluorescent reporters.

Methods

Transgenic lines

Based on cytological examination of promoter:reporter constructs of promoters reported to be specific to the various cell types in the *Arabidopsis* embryo sac (Steffen et al. 2007; Yang et al. 2005), a number of promoters suitable for cell-type-specific expression were identified. Genomic sequences upstream of *DOWN REGULATED IN DETERMINANT INFERTILE 1 (DD)* genes *DD1*, *DD2*, *DD31*, *DD45*, *DD65*, as well as *At1g29140*, *At4g21630*, cytochrome P450, family 86, subfamily C, polypeptide 1 (*CYP86C1*), *Arabidopsis thaliana RWP-RK domain-containing protein 2 promoter* (RKD2), and *At5g49180* genes were PCR amplified from *Arabidopsis* Col-0 DNA. A synthetic $EASE_{pro}$ was constructed and was similar in sequence to the synthetic promoter produced by Yang et al.

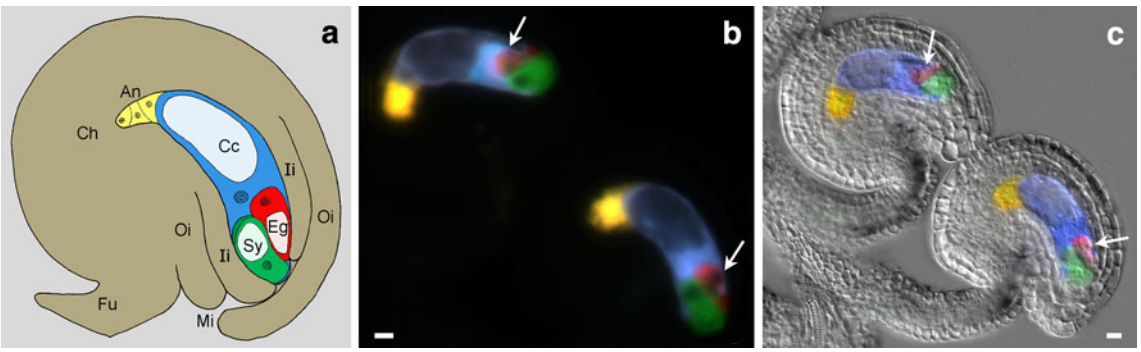

Fig. 1 **a** Pictorial representation of an *Arabidopsis* ovule at the mature female gametophyte stage of development. A single unfertilized egg cell (Eg, *red*) is shown at the micropylar end (Mi) of the egg sac along with two synergid cells (Sy, *green*). A large central cell (Cc, *blue*) contains a secondary nucleus, the product of the fused polar nuclei, and a large vacuole. Three antipodal cells (An, *yellow*) are at the chalazal (Ch) end of the egg sac. The inner- (Ii) and outer-integuments (Oi) surround the embryo sac, and the ovule is anchored to the gynoecium and supplied with nutrients through the funiculus (Fu). **b** Fluorescent micrograph of transgenic ovules visualized with quadruple-labeled expression cassettes at the mature female gametophyte stage demonstrating the cell-specific promoter-fluorescent protein labeling of the antipodals (ZsYellow), the central cell (AmCyan), the egg cell (DsRed, *arrows*), and synergid cells (AcGFP). **c** Fluorescent-labeled embryo sacs from **b** overlaid onto a differential interference contrast (DIC) image of the ovules. Eggs indicated by *arrows*. *Bars* 10 μM

(2005). Each promoter was verified by complete sequencing and inserted into Gateway compatible vectors to drive gene expression of *β-glucuronidase* or fluorescent protein reporter sequences. Sequence-confirmed expression cassettes (Table 1) were transformed into *Agrobacterium tumefacians* strain GV3101 for use in plant transformations. *Arabidopsis thaliana* ecotype L*er* plants were grown, transformed, and selected as previously described (Lawit et al. 2010). When seed fluorescence was used as the selectable marker, a Union Biometrica COPAS Plus system (Boston, MA) was used to perform fluorescence-assisted seed sorting (Schneider 2003). Fluorescent protein-coding sequences were utilized under license from Clontech (Mountain View, CA).

Synergid and egg cell ablation

In order to produce lines with functional ablation and fluorescent markers, we found it necessary to transform the barnase toxin-expressing constructs into lines constitutively expressing the barnase resistance gene, barstar (*GmEF1α$_{pro}$:barstar*). These barstar maintainer plants preserved their hemizygous state through multiple generations through a linked pollen ablation transcriptional unit (*At1g29140$_{pro}$:DAM methylase*) to prevent paternal transgene transmission and allow segregating seed to be sorted via a red fluorescent seed color marker (*RD29A$_{pro}$:DsRed-Express*).

Cytology

Flowers and young siliques were harvested and immediately placed in either phosphate buffered saline (PBS; pH7.2) or in 2 % paraformaldehyde (Electron Microscopy Sciences, Hatfield, PA) in PBS on ice. Ovules were dissected out of the gynoecium or siliques and mounted on well slides in PBS for microscopic observations. Material for GUS staining was dissected and placed in the GUS substrate (Emmanuel et al. 2006) under vacuum (10 psi) for 2 h then placed at 37 °C for 48 h. Samples were washed 3X in PBS and then fixed in 2 % paraformaldehyde: 2 % glutaraldehyde (Electron Microscopy Sciences) in PBS overnight at 4 °C. GUS-stained ovules were cleared in a graded 2,2′-thiodiethanol (TDE, Sigma, St. Louis, MO) series (Staudt et al. 2007) and then mounted in 97 % TDE on glass slides. Fresh ovules were stained for callose with 0.005 % aniline blue (Sigma) in 150 mM K_2HPO_4.

Observations and images were taken with a Leica (Wetzlar, Germany) DMRXA epifluorescence microscope with a mercury light source using fluorescence, bright-field, and differential interference contrast (DIC) optics. The fluorescent filter sets used were from Chroma Technology (Bellows Falls, VT); Aqua #31036v2 (exc. 426–446, dichroic 455LP, em. 465–495), Alexa 488 #MF-105 (exc. 486–500, dichroic 505LP, em. 510–530), Alexa 532 #MF-106 (exc. 509–529, dichroic 535LP, em. 541–561), and Cy3 #C-106250 (exc. 541–551, dichroic 560LP, em. 565–605). Images were captured with a Photometrics (Tucson, AZ) CoolSNAP HQ CCD camera and images manipulated by Molecular Devices (Downingtown, PA) MetaMorph imaging software. Some final image manipulations were accomplished with Adobe Systems (San Jose, CA) Photoshop CS.

Accession numbers

Sequence data from this article can be found in the *Arabidopsis* Genome Initiative database under the following genetic loci: *DD1* (At1g36340), *DD2* (At5g43510), *DD31* (At1g47470), *DD45* (At2g21740), *DD65* (At3g10890), *CYP86C1* (At1g24540), RD29A (At5g52310), and *RKD2* (At1g74480).

Material transfers

The transgenic plant materials described in this publication will be made available to not-for-profit entities solely for

Table 1 List of constructs transformed into *Arabidopsis*

Name	Description
Synergid ablation	*NOS$_{pro}$:Bar/EASE$_{pro}$:barnase/DD65$_{pro}$:AmCyan/DD45$_{pro}$:DsRed-Express/DD31$_{pro}$:AcGFP1*
Cell ablation *GUS*-negative control	*NOS$_{pro}$:Bar/DD45$_{pro}$:β-glucuronidase/DD65$_{pro}$:AmCyan/DD45$_{pro}$:DsRed-Express/DD31$_{pro}$:AcGFP1*
Barstar maintainer	*At1g29140$_{pro}$:DAM methylase/GmEF1α$_{pro}$:barstar/RD29A$_{pro}$:DsRed-Express*
Quadruple + embryo label	*DD31$_{pro}$:AcGFP1/DD65$_{pro}$:AmCyan/DD45$_{pro}$:DsRed-Express/DD1$_{pro}$:ZsYellow1/GmKTI3$_{pro}$:AcGFP1*
Quadruple label	*NOS$_{pro}$:Bar/DD31$_{pro}$:AcGFP1/DD65$_{pro}$:AmCyan/DD45$_{pro}$:DsRed-Express/DD1$_{pro}$:ZsYellow1*
DD45$_{pro}$ egg cell ablation	*NOS$_{pro}$:Bar/DD45$_{pro}$:barnase/DD65$_{pro}$:AmCyan/DD45$_{pro}$:DsRed-Express/DD2$_{pro}$:ZsGreen1*
At4G21630$_{pro}$:RKD2	*NOS$_{pro}$:Bar/At4G21630$_{pro}$:RKD2/DD45$_{pro}$:DsRed-Express*
CYP86C1pro:RKD2	*NOS$_{pro}$:Bar/At4G21630$_{pro}$:RKD2/DD45$_{pro}$:DsRed-Express*
At5g49180$_{pro}$:RKD2	*NOS$_{pro}$:Bar/At5g49180$_{pro}$:RKD2*
RKD2$_{pro}$ egg cell ablation	*NOS$_{pro}$:Bar/RKD2$_{pro}$:barnase/DD65$_{pro}$:AmCyan/DD45$_{pro}$:DsRed-Express/DD31$_{pro}$:ZsYellow1*

noncommercial research purposes, upon acceptance and signing of a Pioneer material transfer agreement, and then only in accordance with all applicable governmental regulations. Such plant materials may contain or be derived from materials obtained from a third party, and the transfer to the requestor of such material will be subject to the requisite, prior permission from any third-party owners, licensors, or controllers of all or parts of the material. Obtaining any permissions will be the sole responsibility of the requestor.

Results

Simultaneous fluorescent labeling of specific cell types within the embryo sac

A number of genes with highly specific expression patterns within the *Arabidopsis* ovule have been identified previously (Gross-Hardt et al. 2007; Johnston et al. 2007; Koszegi et al. 2011; Steffen et al. 2007; Yang et al. 2005). These earlier studies showed clear cell-specific expression with *promoter*:*GFP* fusions, and the expression patterns were validated here with both fluorescent reporter fusions and GUS (Supplementary Figure 1). These observations of non-overlapping single-cell labeling led to the concept of visualizing multiple neighboring cells in the same embryo sac using colored fluorescent reporters. Several *Arabidopsis* promoters identified by Steffen et al. (2007) were used in this study, including a number of *DOWN REGULATED IN DETERMINANT INFERTILE 1* gene promoters *(DD#$_{pro}$)*. *DD45$_{pro}$* (Steffen et al. 2007) was fused to *DsRed* to enable monitoring of egg cell development through fertilization and subsequent embryo development to the globular stage. The *DD65$_{pro}$:AmCyan* cassette highlighted the central cell and early endosperm. Synergid cells were observed with *DD2$_{pro}$* or *DD31$_{pro}$* driving *ZsGreen* or *AcGFP*, respectively, before fertilization and persisting through early zygote development. A fusion of *DD1$_{pro}$* to *ZsYellow* was used to visualize antipodal cells at the chalazal end of the embryo sac. The individual reporters when molecularly cloned into four- and three-fluorescent protein cassettes enabled distinct visualization of the different cell types within the embryo sac simultaneously (Fig. 1) and facilitated detailed observations of the embryo sac in live and fixed transgenic ovules.

Developmental observations

Egg Cells and Young Zygotes. On average, we found *Arabidopsis* egg cells to be approximately 26.4 μm tall × 14.8 μm wide just prior to fertilization. The egg cell and early zygote always demonstrated the same polarity, with the majority of the cytoplasm at the chalazal 25–35 % of the cell along with a large nucleus (Figs. 1b, 2a) and a single large vacuole occupied the micropylar 65 % of each cell (Figs. 1b, 2a). Subtended by the synergids, the apex of the egg/zygote rose just above the synergids. We found eggs to be preferentially localized to the abaxial side of the embryo sac 66 % ($n = 123$) of the time. In a given silique, all eggs showed the same position, either ab- or adaxial. As the post-fertilization zygote elongated, we observed the large central vacuole disappearing while the zygote filled with cytoplasm (Fig. 2b–d). The zygote then elongated and the single nucleus was located at the apex of the proembryo (Fig. 2d). The first division of the embryo was anticlinal and asymmetric, producing a small apical and large elongate basal cells (Fig. 2e). The basal cell divided first and asymmetrically to produce a 3-celled embryo (Fig. 2f). The two apical-most cells then differentiated into the embryo proper and root-cap, respectively, (reviewed by Laux et al. 2004), and the basal-most cell became the suspensor. The apical cell was observed to undergo two periclinal divisions to produce a four-celled embryo proper (Fig. 2g, h), and cells of the suspensor then elongated and pushed the four-celled embryo proper further into the endosperm (Fig. 2i).

Central cell and early endosperm. In a study of the developmental progression of the central cell and endosperm, we report a summary of observed cell divisions, migrations, and patterns of development (Fig. 3). At cellularization of the female gametophyte, the two haploid polar nuclei occupied a position adjacent to and just chalazal to the egg (Fig. 3a and Supplementary Fig. 3d). The polar nuclei then fused prior to fertilization (Fig. 3b) to become the secondary nucleus. The diploid secondary nucleus remained positioned near the apex of the egg, possibly facilitating the fertilization of both cells upon release of sperm from the pollen tube. The remainder of the central cell was composed of a large central vacuole and a thin layer of cytoplasm along the central cell wall (Figs. 1, 3b). We observed swelling of the primary endosperm nucleus prior to the first division, which reached up to 16.0 μm in diameter with a nucleolus up to 7.2 μm in diameter (Fig. 3c). After division, the triploid endosperm nuclei were still larger (up to 6.5 μm in diameter) than the nucleus of the egg/zygote. The first division of the primary endosperm nucleus precedes that of the zygote (Fig. 3d).

After the first division of the primary endosperm nucleus, one nucleus was observed to migrate chalazally within the central cell while the sister nucleus remained in close proximity to the zygote apex (Fig. 3e). Both endosperm nuclei divided, and the first four endosperm nuclei were equally spaced along the length of the embryo sac (Fig. 3f). At the four-nucleate endosperm stage, the chalazal-most nucleus migrated to the extreme end of the

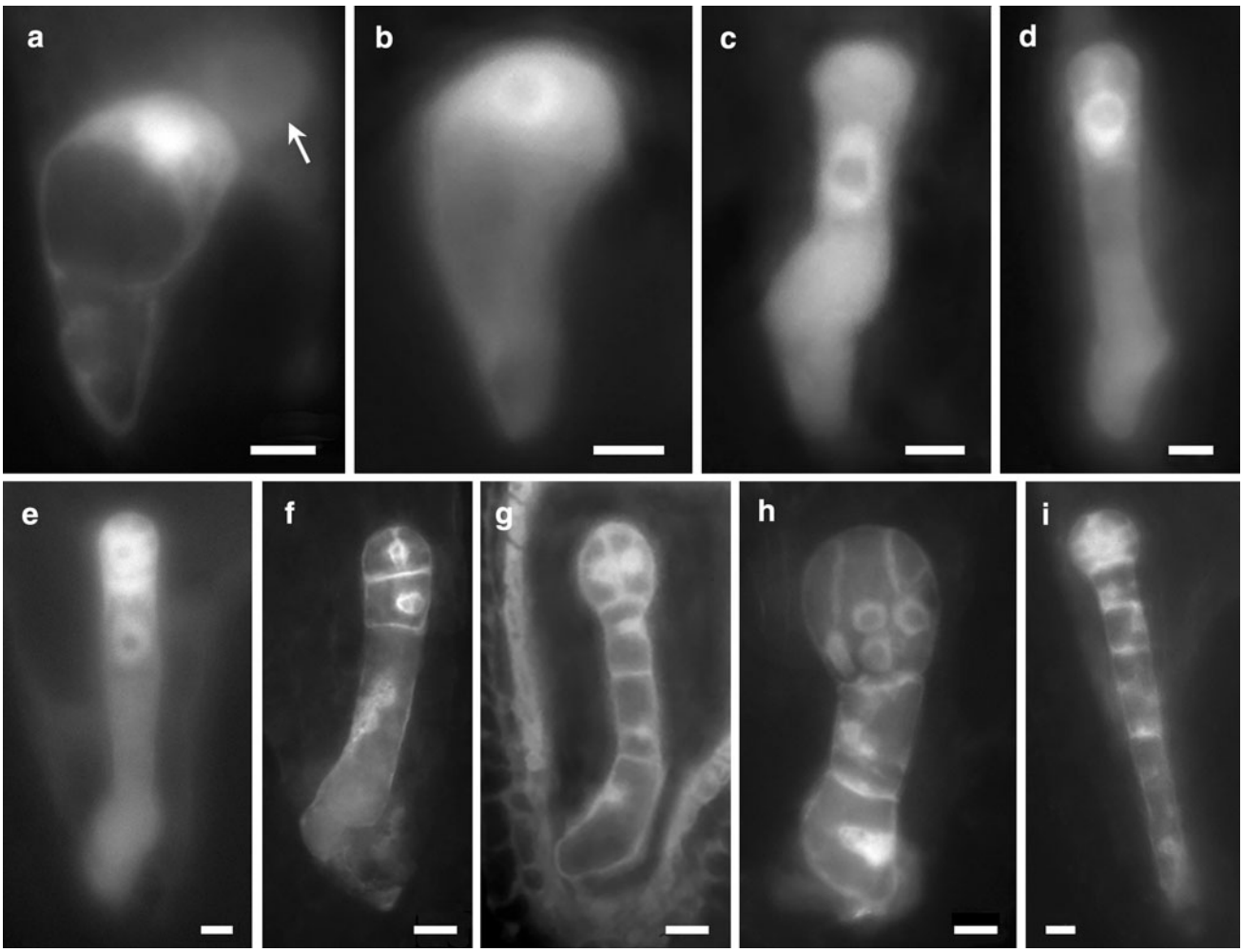

Fig. 2 *Arabidopsis* early embryo development as detected by *DD45*$_{pro}$*:DsRed-Express* fluorescence expression. **a** Zygote and primary endosperm nucleus (*arrow*) shortly after fertilization—with nucleus and the bulk of the cytoplasm occupying the apical end of the zygote. **b** Zygote enlarged and less vacuolated. **c, d** Elongated, torpedo-shaped zygote. **e** A small apical and large basal cells resulting from an asymmetric anticlinal division. **f** Basal cell divided asymmetrically to produce a 3-celled embryo. The two apical-most cells will become the embryo proper and root-cap, respectively, (reviewed by Laux et al. 2004), and basal-most cell will develop into the suspensor. **g, h** Two periclinal divisions of the apical cell producing a four-celled embryo proper. **i** Eight-celled embryo resulting from elongation of suspensor cells pushing the four-celled embryo proper further into the endosperm. *Bars* 10 μm

embryo sac (Fig. 3g). This nucleus enlarged and became surrounded by dense cytoplasm (Fig. 3h). Divisions of this chalazal nucleus were delayed while the other three endosperm nuclei continue to divide synchronously for three or four cycles. In the four-nucleate proembryo/16-free-nucleate endosperm stage, the chalazal endosperm plug began to form (Fig. 3h, i). Initially, only two nuclei and associated dense cytoplasm comprised the plug; these nuclei were larger (7.9–8.1 μm) than those in the rest of the embryo sac (5.6–6.8 μm). The absence of karyokinesis of these chalazal nuclei likely resulted in endoreduplication as suggested by their increased size and density, similar to that noted by (Ingouff et al. 2005). By the proembryo stage, a significant chalazal endosperm plug resembling a small globular embryo was present, measuring 31.5 μm tall × 19.7 μm wide (Fig. 3j). This plug was composed of densely compacted cytoplasm with up to 12 nuclei. The chalzal plug was negative for callose staining. Its' increased surface area suggests a conduit for nutrient flow into the embryo sac. The uniqueness of the chalazal region and its role in channeling photosynthates into the embryo sac during early embryo development has been shown in soybean ovules (Chamberlin et al. 1993).

The endothelial layer (innermost layer of inner integument) differentiated during the early globular embryo stage, and the endothelial cells began to fill with opaque oil-like bodies (not shown). These structures were highly autofluorescent (Fig. 3j) and consequently obscured imaging of the endosperm and embryo at later stages of development.

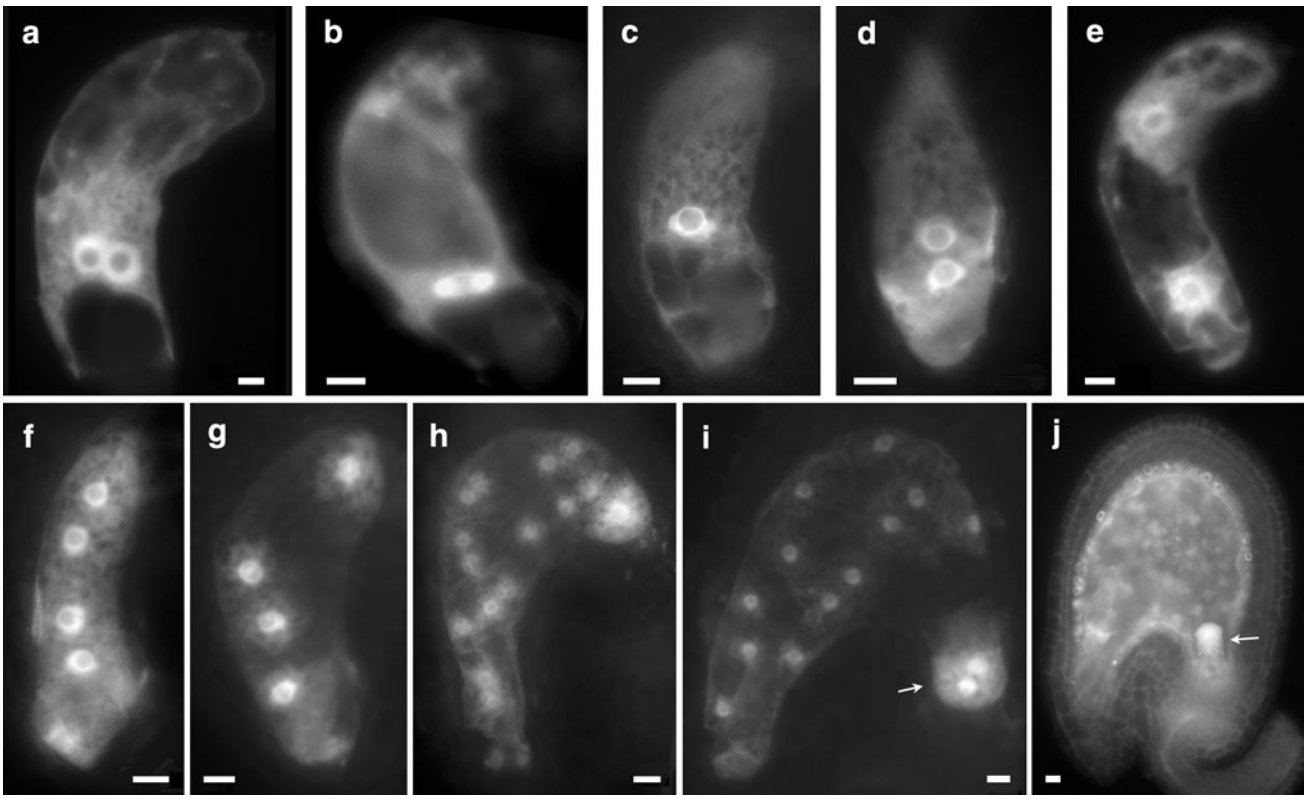

Fig. 3 Progression of central cell and endosperm development in micrographs of transgenic ovules visualized with quadruple-labeled expression cassettes. Micrographs highlight the central cell with cell-specific promoter-fluorescent protein labeling (*DD65$_{pro}$:AmCyan*). Ovules are shown to progress from the mature female gametophyte stage (**a**) through late heart stage embryo development (**j**). **a** Two haploid polar nuclei are visible in the central cell just prior to fusion, and **b** during nuclear fusion where the central cell had a large central vacuole. **c** The central cell nucleus swelled and moved chalazally prior to the first division (**d**). **e** One of the two resulting nuclei migrated chalazally to the middle of the central cell. **f** Following the second division, the four endosperm nuclei were equally spaced within the embryo sac. **g** One nucleus translocated to the chalazal pole of the endosperm and was surrounded by dense cytoplasm, as the remaining nuclei were distributed evenly (**h**). In the 16-nucleate uncellularized endosperm stage, the chalazal endosperm plug began to form (*arrow*) (**h, i**). **j** At the proembryo stage, a significant chalazal endosperm plug was observed (*arrow*). Endothelial layer showed significant autofluorescence, likely a result of lipid accumulation. *Bars* 10 μm

Synergids. *DD2$_{pro}$*, and *DD31$_{pro}$* expression patterns (Fig. 1; Supplementary Figs. 1b-c) were consistent with the characterization performed by Steffen et al. (2007). Just prior to fertilization, the synergids were uniform in size at approximately 28.0 μm tall and 15.0 μm wide, which is slightly larger than the egg (approx. 26.5 μm tall and 15.0 μm wide). The filiform apparatus (Huang and Russell 1992) occupied the basal 20 % of the synergids, and a large vacuole (40–50 % volume of the cell) was seen at the apex of the synergid cells at fertilization. No significant dimorphism was noted between the two synergid cells, both had a large vacuole at their apex with the majority of the cytoplasm and the nucleus occupying the basal half of each cell (Supplementary Fig. 2). The synergid nuclei were roughly the same size as the egg cell nucleus. The synergids were morphologically distinct from the egg cell, and their cellular contents (nucleus, cytoplasm, and large vacuole) are polar opposites by comparison. After pollen tube penetration and fertilization, the degenerate synergid showed signs of cytoplasmic condensation and began to collapse. The persistent synergid remained intact and did not begin to break down (loss of vacuole and cytoplasmic condensation) until after the first division of the zygote. Interestingly, a remnant of the persistent synergid was often still fluorescent at the early proembryo (four-nucleate) stage (not shown). Cellular and positional identity within the female gametophyte appears to be determined early in development as evidenced by *DD31$_{pro}$:β-glucuronidase* expression that was noted at the extreme micropylar end of the developing embryo sac as early as the 4-nucleate stage of megagametogenesis (not shown). *EASEpro:ZsGreen1* expression was observed to be strongly synergid preferred (Supplementary Fig. 2).

Antipodals. Antipodals were observed to differentiate prior to the egg and synergids, and *DD1$_{pro}$:ZsYellow* expression was only detected after antipodal nuclei took their chalazal positions and formed cell walls (Supplementary Figs. 3a-c). Antipodal differentiation clearly

occurred prior to the egg and synergid differentiation and cellularization (Supplementary Fig. 3d). The early establishment of antipodals, relative to the egg and synergids, and their close physiological connection with the nucellar cells suggests that the antipodals play an early role in nutritional transport into the developing female gametophyte. The antipodal cells typically measured 5–9 μm on average, but were up to 14.6 μm in diameter. At the first stages of antipodal differentiation, the *DD1$_{pro}$:ZsYellow* reporter was expressed only in the three antipodals; however, in some ovules, more than three cells fluoresced as development progressed. Upon close examination, the extra fluorescing cells were determined to be nucellar cells and not antipodals. This radiating fluorescence was up to three cell layers deep around the antipodals, resulting in tens of fluorescent nucellar cells around the antipodals. It appears that this expression resulted from symplastic movement of the fluorescent protein or its mRNA in a cell-to-cell manner from the antipodals to the nucellus. Surprisingly, no *DD1$_{pro}$:ZsYellow* fluorescence was observed in the central cell adjacent to the antipodals. This suggests that the antipodals have symplastic connections with the nucellar cells, but not with the central cell with which they share a direct lineage, the female gametophyte (Supplementary Figs. 3d-f).

Targeted ablation of synergids

Cell-specific synergid ablation was demonstrated using the toxin barnase driven by an artificial promoter containing the *Egg Apparatus Specific Enhancer*, *EASE$_{pro}$* (Yang et al. 2005), referred herein as the synergid ablation construct (Table 1). Expression of barnase is lethal to plant cells. Ablation was compared with a cell ablation *GUS*-negative control construct, and cell fate was monitored using zygote/central cell/synergid triple fluorescent-labeled embryo sac cells. The cell ablation *GUS*-negative control demonstrated that co-expression of an additional non-toxic gene in one of the labeled cell types did not disrupt the embryo sac (Fig. 4a). Our first attempt at transformation of the synergid ablation expression cassette into wild type *Arabidopsis* was not successful. *Agrobacterium* floral dip transformation of *Arabidopsis* occurs in female tissues approximately 5 days before pollination (Desfeux et al. 2000). Therefore, embryo sac cell ablation expression cassettes, if active, would inhibit transgenic embryo development, explaining the lack of successful transformation. In order to alleviate the transformation difficulties and prevent any potential toxic effect of barnase misexpression on non-targeted cells and tissues, we produced a perpetually hemizygous transgenic line widely expressing the barnase anti-toxin, barstar (Hartley 1988). The barstar maintainer cassette segregated in the female germ line, but did not transmit through the male due to a male gametophyte ablation cassette. Expression of barstar (Hartley 1989) was driven by the soybean *GmEF1α$_{pro}$*, resulting in strong expression in all transgenic tissues of the plants. With super transformation into the *GmEF1α$_{pro}$:barstar* background, representative transgenic ovules with the synergid ablation cassette showed clear synergid absence, 8 % of more than 600 ovules from 17 lines (Fig. 4b–d; Supplementary Figs. 4a-b). Egg cell expression was apparent in some synergid ablation lines. Mild degrees of egg cell and central cell perturbation were observed in 12 % of the ovules (Supplementary Fig. 4c). Relatively, few lines showed egg cell ablation alone (<1 %), while others demonstrated both egg cell and synergid ablation (2 %).

Targeted ablation of egg cells

Similar to the approach with synergid ablation, egg cell ablation constructs were produced to induce and to follow the events of egg cell ablation. The *DD45$_{pro}$*- and *RKD2$_{pro}$*-egg cell ablation constructs were transformed into the hemizygous *barstar maintainer* genetic background. Representative ovules showed clear absence of an egg cell and little or no perturbations in the synergids and central cell (Fig. 5a–d), indicating that the toxin selectively targeted the egg alone. Most *DD45$_{pro}$* egg cell ablation lines showed a variety of morphological irregularities (Supplementary Fig. 5). Approximately 4 % of the >700 ovules examined from five *DD45$_{pro}$* egg cell ablation lines showed egg cell ablation without obvious morphological defects in the synergids or central cell. Egg cell ablation without morphological irregularities was more frequently observed with *RKD2$_{pro}$* egg cell ablation cassettes, 12 % of >780 ovules from 18 lines (Fig. 5c, d). Several *RKD2$_{pro}$* egg cell ablation lines had developing endosperm (Fig. 5e, f) and produced mature, embryo-less, shrunken seed (Fig. 5g), demonstrating successful targeted ablation of egg cells.

Transdifferentiation of synergid cells to egg or zygote-like structures was observed in some egg cell ablated ovules (Fig. 6; Supplementary Fig. 5d). Upon ablation and loss of the egg, the synergids in these cases became morphologically similar to a normal egg/zygote. The synergids changed cytoplasmic and nuclear polarity to become more egg/zygote-like, with the nucleus and bulk of the cytoplasm taking an apical position, while the single large vacuole moved basipetally. These transdifferentiating synergids also expressed the identity markers of both the egg (*DD45$_{pro}$*) and synergid (*DD31$_{pro}$*), indicating a mixed cell fate. The position within the embryo sac of these dual identity cells was similar to that of an egg or zygote in a normal ovule. Those cells in the typical location of synergids were either completely absent, or only a single synergid was present. Of the approximately >125 ovules

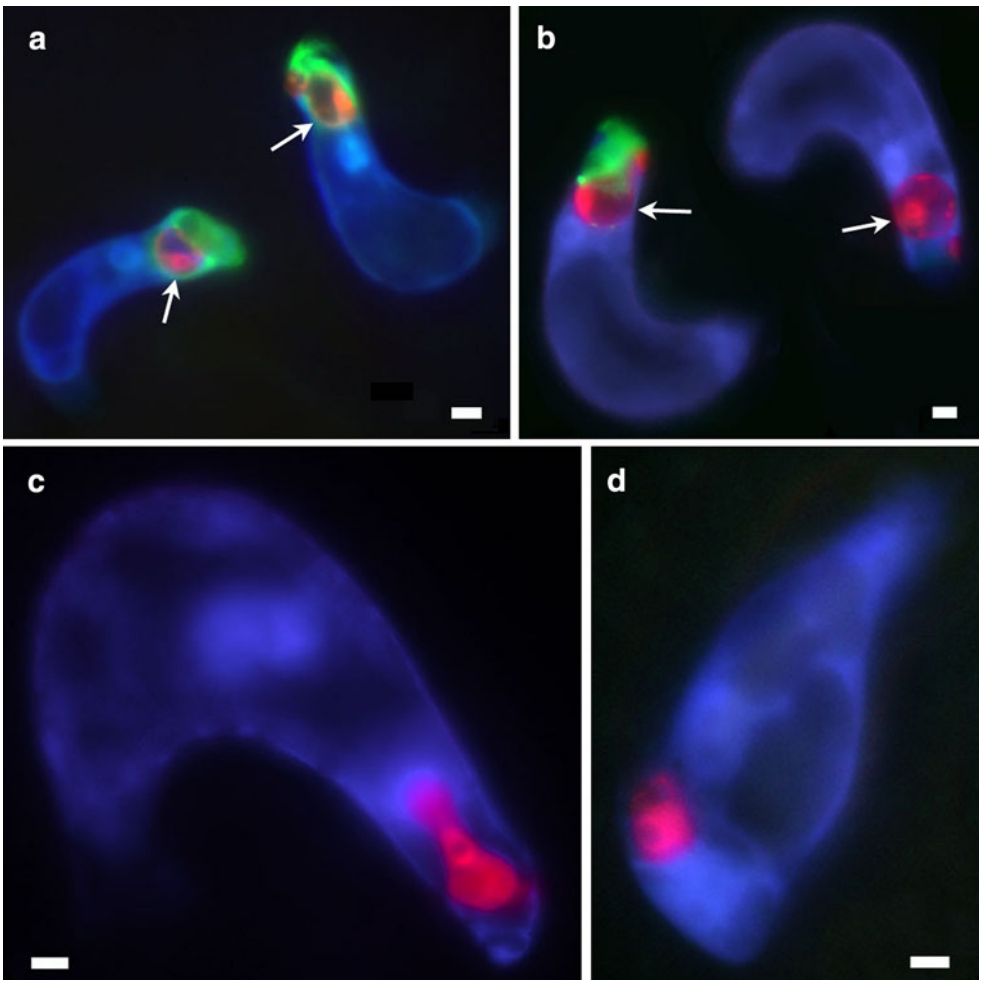

Fig. 4 Transgenic ovules co-expressing a synergid ablation, and triple fluorescent-labeled expression cassettes to monitor egg/zygote (*DsRed*), synergids (*AcGFP*), and central cell (*AmCyan*) development. **a** Cell ablation negative control ovules showing two stages of normal development demonstrate viability of constructs expressing non-toxic genes. Ovule at *left* (pre-fertilization) shows a mature embryo sac with an egg, synergids, and central cell. Ovule at *right* (post-fertilization) is similar to the embryo sac at *left*, but shows the breakdown of the degenerate synergid (*green*) following pollen tube penetration. **b** Representative synergid ablation transgenic ovules segregating for the *barstar* maintainer expression cassette. Ovule at *left* shows normal development of the embryo sac. On the *right*, synergid ablation has occurred, but the zygote and central cell appear to have been fertilized and were developing normally. **c** and **d** Representative transgenic synergid ablation ovules post-fertilization showing an absence of the synergids, somewhat abnormal shaped zygotes and normal central cell development. Egg or zygote (*red*) indicated by an *arrow*. *Bars* 10 μm

that had a clear loss of the egg/zygote and appeared healthy, 15 % showed the above synergid-egg transitional pattern. In rare instances, both the synergid and egg markers were observed later in development in the embryo at the globular stage (Fig. 6d). In these unique events of synergids transitioning to embryos, it appears that fertilization did occur. The degenerate synergid was absent and endosperm development was observed, suggesting that at least fertilization of the secondary nucleus occurred. Whether fertilization of either of the sexual egg had occurred followed by abortion, or that one of the synergids was fertilized in the absence of the egg is unknown. Events were rare in which a synergid transitioned to an embryo of sufficient maturity for cytological analysis. Therefore, examining the ploidy level of the transdifferentiated synergids to determine whether they are haploid (unfertilized) or diploid (fertilized) is not practical at this time.

RKD2-induced adventitious embryo-like structures

A requirement of apomictic reproduction is the formation of an embryo within the ovule without fertilization, and we developed ablation and monitoring constructs to achieve this goal. To facilitate detection of egg-, zygote-, or embryo-like structures, $DD45_{pro}$*:DsRed-Express* was included in our expression cassette, or the construct was super transformed into the quadruple + embryo label genetic background expressing four distinct fluorescent

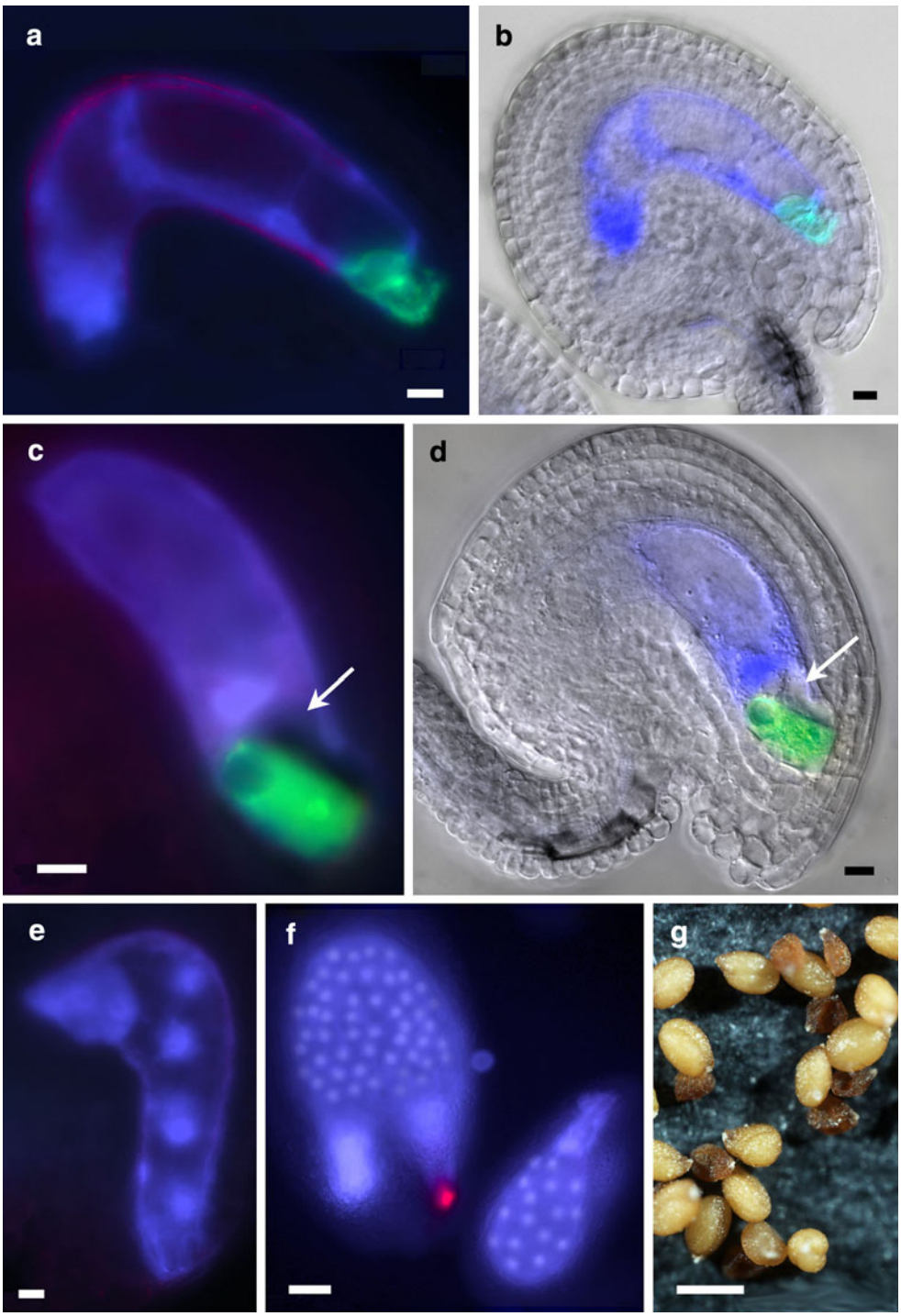

Fig. 5 Transgenic ovules and mature seed expressing egg cell ablation cassettes. **a** and **b** Post-fertilization ovule from the $DD45_{pro}$ egg cell ablation construct with the persistent synergid (*green*) and normal development of the central cell, no egg, or zygote present; **a** fluorescence and **b** fluorescence/DIC overlay. **c–g** $RKD2_{pro}$ egg cell ablation ovules at various stages of development. **c** and **d** Fluorescence and fluorescence/DIC images of an ovule at the egg cell stage. Egg is absent and only a void remained (*arrows*) while the synergids and central cell appeared normal in development. **e** and **f** Ovules at different stages showing endosperm development evident by numerous endosperm nuclei (*bright blue spots*). Remnant of an embryo (*red*) visible in embryo sac at *left* (**f**). Absence of a developing embryo correlated with a shrunken seed phenotype (**g**). **a–e** *Bars* 10 μm, **f** *Bar* 50 μm and **g** *Bar* 500 μm

proteins labeling individual cell types within the embryo sac. Numerous promoters were tested for their ability to target expression to somatic maternal-only tissues in ovules (Supplementary Fig. 6). Selected promoters were then utilized to complement embryogenic-type coding sequence combinations to test for induction of novel embryogenesis

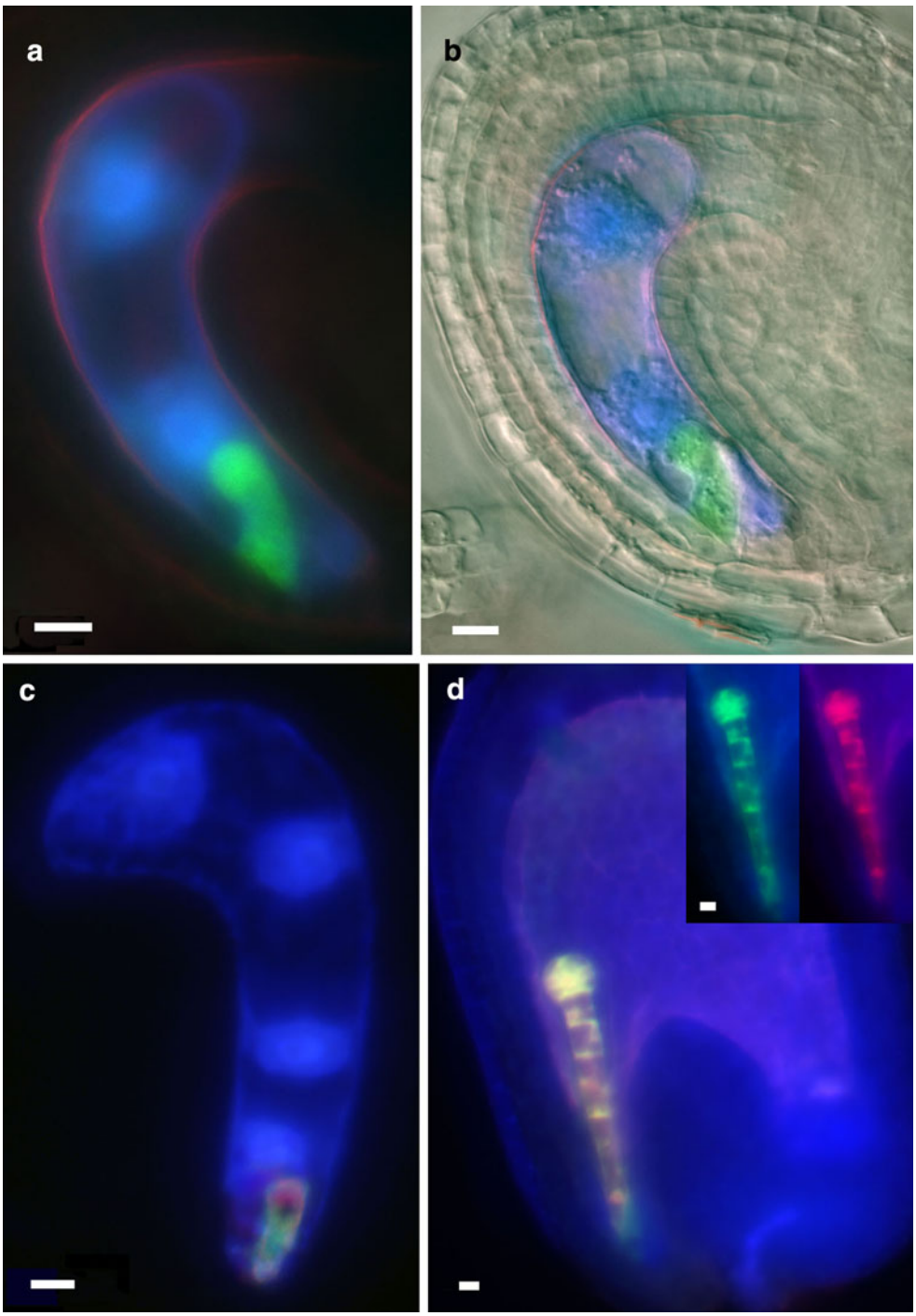

Fig. 6 Fluorescent micrographs of transgenic ovules showing changes in cell fate specificity after egg cell ablation. **a, b** The egg/zygote was ablated by the $DD45_{pro}$ egg cell ablation cassette while the endosperm appeared normal. The persistent synergid became zygote-like in morphology, but still retained the synergid fluorescent marker ($DD31_{pro}$*:AcGFP*). **c** A zygote from an $RKD2_{pro}$ egg cell ablation line, and **d** a globular embryo expressing the $DD45_{pro}$ egg cell ablation cassette share both the *green* synergid and *red* egg cell $DD45_{pro}$*:DsRed-Express* color markers (insets), suggesting a mixed cell identity. *Bars* 10 μm

from somatic ovular tissue (Supplementary Fig. 7). The expression of RKD2 from an ovule maternal tissue–specific promoter, $At5g49180_{pro}$ or *CYP86C1pro*; led to the induction of the egg/embryo $DD45_{pro}$*:DsRed-Express* reporter in multiple cells outside of the embryo sac in the integuments. (Fig. 7a, b; Supplementary Figs. 7a and d). Approximately, 10 % of the ovules showed a $DD45_{pro}$*:DsRed-Express* reporter-positive response in the integumentary cells of >1,800 and >900 ovules, respectively. Many of these cells became enlarged, densely

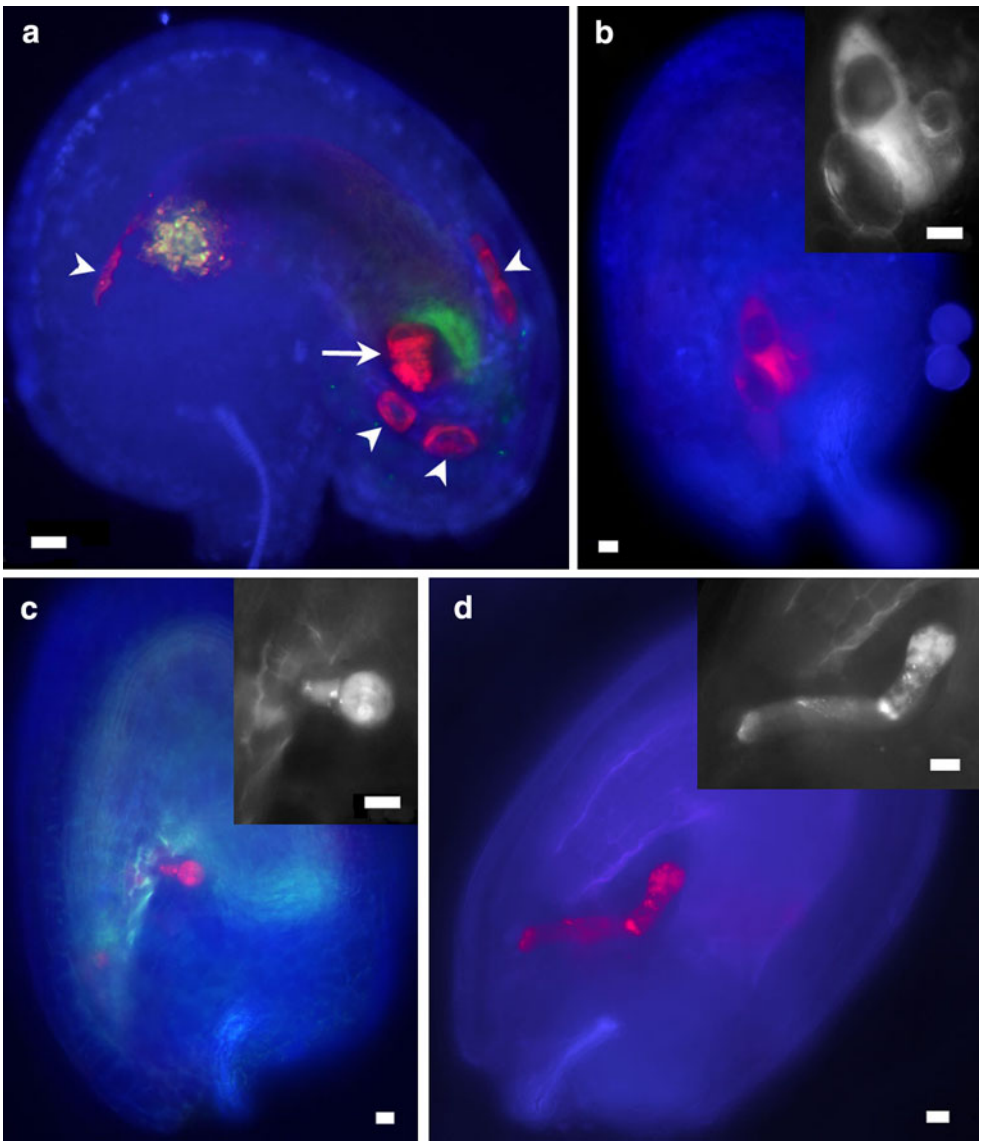

Fig. 7 Fluorescent micrographs of transgenic ovules ectopically expressing the RKD2 transcription factor in sporophytic cells showed adventitious egg cells or embryos. **a** An ovule carrying the *At5g49180*$_{pro}$*:RKD2* transgene, in a quadruple label genetic background. Several cells (*arrowheads*) outside of the embryo sac became swollen and densely cytoplasmic and expressed the egg cell marker, *DD45*$_{pro}$*:DsRed-Express*. *Arrow* native egg. **b** A *CYP86C1*$_{pro}$*:RKD2* transgenic ovule carrying *DD45*$_{pro}$*:DsRed-Express* egg/embryo fluorescent marker. Three cells of the integuments immediately outside the micropylar end of the embryo sac became enlarged and expressed the egg/embryo marker. The *center* cell appeared morphologically similar to a zygote. **c** and **d** *At4G21630*$_{pro}$*:RKD2* transgenic ovules containing the *DD45*$_{pro}$*:DsRed-Express* reporter. Young globular stage embryos were visible outside of the embryo sac and in **c** appeared to originate from the maternal tissue (inner integuments) immediately outside the embryo sac. *Bars* 10 μm

cytoplasmic and had a prominent nucleus, indicating pluripotency (meristematic activity). Ectopic expression of RKD2 from *At4G21630*$_{pro}$ (Supplementary Figs. 7b-c) produced similar results, with fewer expressing cells. In 3–4 rare events (ca. 0.1 %), embryo-like structures were observed outside of the embryo sac, suggesting that *RKD2*-mediated embryogenesis from maternal tissues of the ovules (Fig. 7c, d). In no observations of more than 40,000 ovules from other transgenic cassettes have similar morphological changes been noted in maternal tissues.

Discussion

The creation of the cell-specific multi-labeled embryo sacs described here has facilitated observations demonstrating novel manipulations of plant reproductive biology. This visual marker system enables tracking of the effects of development and cell-specific manipulations on each cell type of the embryo sac and on the embryo sac as a whole.

The ability to specifically ablate synergid or egg cells through a transgenic method without leading to other

gametophyte defects has been demonstrated. Targeted cell ablation early in reproductive cell lineages and in the embryo sac is of interest for both academic (Koltunow et al. 2011; Yang et al. 2005) and applied purposes. Our results show the clear capacity for decoupling of the embryo from endosperm development in *Arabidopsis*. This is in contrast with the suggestions of Völz et al. (2012), where egg cell- and early embryo-targeted RNA-interference of the *LACHESIS* gene resulted in developmental abnormalities in the entire female gametophyte. The discrepancy in results suggests that the observations of Völz et al. (2012) may be more related to functions of the *LACHESIS* gene product than to more general cellular functions of the egg cell in embryo sac development, at least after fertilization. This opens up a number of potential applications including prevention of sexual embryo formation.

Although ablation lines with no unintended developmental abnormalities were observed, some results suggest a native plasticity of synergid cell identity. In some lines, a synergid marker, in addition to the egg marker, was found in egg-, zygote-, and embryo-like structures. Such results are not unprecedented. Ovules with a mutation in the *VERANDI* gene demonstrated a misspecification or incomplete differentiation of synergid cells, which commonly began expressing an antipodal cell marker (Matias-Hernandez et al. 2010). Ovules with a mutation in the *LACHESIS* gene also lost gametic cell fate specificity and synergids began expressing egg cell molecular and morphological markers (Gross-Hardt et al. 2007). Similar results have occurred with misexpression of a BEL1-like homeodomain 1 protein in the *eostre* mutant (Pagnussat et al. 2007). In maize, RNAi down-regulation of *Zea mays EA1-like 1* resulted in some antipodal cells changing into central cells (Krohn et al. 2012). Taken together, these results suggest that a number of mechanisms have the potential to alter synergid and egg cell specification. Our observations of cell identity transdetermination in the embryo sac appear to be the first known occurrence without misexpression of a particular developmental gene or pathway. However, these results are consistent with the model that the egg cell is the primary organizer of cell fate and maintenance during the late stages of gametogenesis (Krohn et al. 2012; Völz et al. 2012).

The harnessing of apomixis to create clonal embryos through seed is a potentially potent tool for sustained improvements in agricultural productivity (Ranganath 2011). Adventitious embryony is one of several mechanisms through which clonal embryos may be formed. Previous work has identified genes capable of inducing somatic embryogenesis from differentiated leaf (Boutilier et al. 2002; Ouakfaoui et al. 2010) or root tissue (Wang et al. 2009; Zuo et al. 2002). The work herein demonstrates synthetically induced adventitious embryo-like structures (somatic embryogenesis from ovule tissues). Using the $DD45_{pro}$*:DsRed-Express* reporter as a tool for identifying novel egg, zygote, and early embryo initiation, we found cytological evidence of *RKD2*-induced adventitious embryo-like structures. It is not immediately clear if these adventitious embryo-like structures arise parthenogenetically or via fertilization of an adventitious egg cell by a sperm cell. Low embryo induction rates preclude a definitive molecular study of progeny. In any case, RKD-family proteins (Koszegi et al. 2011) warrant future investigation for induction of totipotency.

Our results add to a rapidly moving field of study. Synthetic sexual embryo prevention and adventitious embryony, as well as multiplexed fluorescent cell markers expand on the rapidly growing tool kit available in the field of plant reproductive biology. These and other recent advances are beginning to unleash new possibilities for crop improvement including the long-sought goal of self-reproducing hybrids.

Acknowledgments The authors would like to thank Ueli Grossniklaus and Tim Bourett for discussions and advice, and Tim Fox and Olga Danilevskaya for critical evaluation of the manuscript. We thank Rachel Huegel, David Oneal, and Susan Wagner for technical assistance.

References

Berger F, Twell D (2011) Germline specification and function in plants. Annu Rev Plant Biol 62:461–484

Berger F, Hamamura Y, Ingouff M, Higashiyama T (2008) Double fertilization-caught in the act. Trends Plant Sci 13:437–443

Boutilier K, Offringa R, Sharma VK, Kieft H, Ouellet T, Zhang L, Hattori J, Liu C-M, van Lammeren AAM, Miki BLA, Custers JBM, van Lookeren Campagne MM (2002) Ectopic expression of BABY BOOM triggers a conversion from vegetative to embryonic growth. Plant Cell 14:1737–1749

Chamberlin MA, Horner HT, Palmer RG (1993) Nutrition of ovule, embryo sac, and young embryo in soybean: an anatomical and autoradiographic study. Can J Bot 71:1153–1168

Cheng C-Y, Mathews DE, Eric Schaller G, Kieber JJ (2013) Cytokinin-dependent specification of the functional megaspore in the *Arabidopsis* female gametophyte. Plant J, pp 929–940

Crismani W, Girard C, Mercier R (2013) Tinkering with meiosis. J Exp Bot 64:55–65

Desfeux C, Clough SJ, Bent AF (2000) Female reproductive tissues are the primary target of *Agrobacterium*-mediated transformation by the *Arabidopsis* floral-dip method. Plant Physiol 123:895–904

Emmanuel E, Yehuda E, Melamed-Bessudo C, Avivi-Ragolsky N, Levy AA (2006) The role of AtMSH2 in homologous recombination in *Arabidopsis thaliana*. EMBO Rep 7:100–105

Gross-Hardt R, Kagi C, Baumann N, Moore JM, Baskar R, Gagliano WB, Jurgens G, Grossniklaus U (2007) LACHESIS restricts gametic cell fate in the female gametophyte of *Arabidopsis*. PLoS Biol 5:e47

Hartley RW (1988) Barnase and barstar. Expression of its cloned inhibitor permits expression of a cloned ribonuclease. J Mol Biol 202:913–915

Hartley RW (1989) Barnase and barstar: two small proteins to fold and fit together. Trends Biochem Sci 14:450

Higashiyama T, Yabe S, Sasaki N, Nishimura Y, Miyagishima S, Kuroiwa H, Kuroiwa T (2001) Pollen tube attraction by the synergid cell. Science 293:1480–1483

Huang B-Q, Russell SD (1992) Female germ unit: organization, isolation, and function. In: Scott DR, Christian D (eds) International review of cytology. Academic Press, pp. 233–293

Ingouff M, Haseloff J, Berger F (2005) Polycomb group genes control developmental timing of endosperm. Plant J 42:663–674

Ingram G (2010) Family life at close quarters: communication and constraint in angiosperm seed development. Protoplasma 247: 195–214

Johnston A, Meier P, Gheyselinck J, Wuest S, Federer M, Schlagenhauf E, Becker J, Grossniklaus U (2007) Genetic subtraction profiling identifies genes essential for *Arabidopsis* reproduction and reveals interaction between the female gametophyte and the maternal sporophyte. Genome Biol 8:R204

Koltunow AM, Johnson SD, Rodrigues JC, Okada T, Hu Y, Tsuchiya T, Wilson S, Fletcher P, Ito K, Suzuki G, Mukai Y, Fehrer J, Bicknell RA (2011) Sexual reproduction is the default mode in apomictic *Hieracium* subgenus *Pilosella*, in which two dominant loci function to enable apomixis. Plant J 66:890–902

Koszegi D, Johnston AJ, Rutten T, Czihal A, Altschmied L, Kumlehn J, Wust SE, Kirioukhova O, Gheyselinck J, Grossniklaus U, Baumlein H (2011) Members of the RKD transcription factor family induce an egg cell-like gene expression program. Plant J 67:280–291

Krohn NG, Lausser A, Juranic M, Dresselhaus T (2012) Egg cell signaling by the secreted peptide ZmEAL1 controls antipodal cell fate. Dev Cell 23:219–225

Laux T, Wurschum T, Breuninger H (2004) Genetic regulation of embryonic pattern formation. Plant Cell 16(Suppl):S190–S202

Lawit SJ, Wych HM, Xu D, Kundu S, Tomes DT (2010) Maize DELLA proteins dwarf plant8 and dwarf plant9 as modulators of plant development. Plant Cell Physiol 51:1854–1868

Li D, Lin M, Wang Y, Tian H (2009) Synergid: a key link in fertilization of angiosperms. Biol Plant 53:401

Marton ML, Cordts S, Broadhvest J, Dresselhaus T (2005) Micropylar pollen tube guidance by egg apparatus 1 of maize. Science 307: 573–576

Matias-Hernandez L, Battaglia R, Galbiati F, Rubes M, Eichenberger C, Grossniklaus U, Kater MM, Colombo L (2010) VERDANDI is a direct target of the MADS domain ovule identity complex and affects embryo sac differentiation in *Arabidopsis*. Plant Cell 22:1702–1715

Ohnishi T, Takanashi H, Mogi M, Takahashi H, Kikuchi S, Yano K, Okamoto T, Fujita M, Kurata N, Tsutsumi N (2011) Distinct gene expression profiles in egg and synergid cells of rice as revealed by cell type-specific microarrays. Plant Physiol 155: 881–891

Olmedo-Monfil V, Duran-Figueroa N, Arteaga-Vazquez M, Demesa-Arevalo E, Autran D, Grimanelli D, Slotkin RK, Martienssen RA, Vielle-Calzada JP (2010) Control of female gamete formation by a small RNA pathway in *Arabidopsis*. Nature 464:628–632

Ouakfaoui SE, Schnell J, Abdeen A, Colville A, Labbé H, Han S, Baum B, Laberge S, Miki B (2010) Control of somatic embryogenesis and embryo development by AP2 transcription factors. Plant Mol Biol 74:313–326

Pagnussat GC, Yu H-J, Sundaresan V (2007) Cell-fate switch of synergid to egg cell in arabidopsis eostre mutant embryo sacs arises from misexpression of the bel1-like homeodomain gene *blh1*. Plant Cell 19:3578–3592

Pagnussat GC, Alandete-Saez M, Bowman JL, Sundaresan V (2009) Auxin-dependent patterning and gamete specification in the arabidopsis female gametophyte. Science 324:1684–1689

Ranganath RM (2011) Developmental switches that hold the key to a revolution in crop biotechnology. Nat Rev Genet 12:224

Sánchez-León N, Arteaga-Vázquez M, Alvarez-Mejía C, Mendiola-Soto J, Durán-Figueroa N, Rodríguez-Leal D, Rodríguez-Arévalo I, García-Campayo V, García-Aguilar M, Olmedo-Monfil V, Arteaga-Sánchez M, Martínez de la Vega O, Nobuta K, Vemaraju K, Meyers BC, Vielle-Calzada J-P (2012) Transcriptional analysis of the *Arabidopsis* ovule by massively parallel signature sequencing. J Exp Botany 63:3829–3842

Schneider I (2003) Novel high-throughput screening technologies: fluorescence. Bioluminescence and flow cytometry aid drug discovery, Genetic Engineering News 23

Sprunck S, Gross-Hardt R (2011) Nuclear behavior, cell polarity, and cell specification in the female gametophyte. Sex Plant Reprod 24:123–136

Sprunck S, Rademacher S, Vogler F, Gheyselinck J, Grossniklaus U, Dresselhaus T (2012) Egg cell-secreted EC1 triggers sperm cell activation during double fertilization. Science 338:1093–1097

Staudt T, Lang MC, Medda R, Engelhardt J, Hell SW (2007) 2,2′-thiodiethanol: a new water soluble mounting medium for high resolution optical microscopy. Microsc Res Tech 70:1–9

Steffen JG, Kang IH, Macfarlane J, Drews GN (2007) Identification of genes expressed in the *Arabidopsis* female gametophyte. Plant J 51:281–292

Sundaresan V, Alandete-Saez M (2010) Pattern formation in miniature: the female gametophyte of flowering plants. Development 137:179–189

Vielle-Calzada JP, Baskar R, Grossniklaus U (2000) Delayed activation of the paternal genome during seed development. Nature 404:91–94

Völz R, von Lyncker L, Baumann N, Dresselhaus T, Sprunck S, Groß-Hardt R (2012) LACHESIS-dependent egg-cell signaling regulates the development of female gametophytic cells. Development 139:498–502

Wang X, Niu QW, Teng C, Li C, Mu J, Chua NH, Zuo J (2009) Overexpression of PGA37/MYB118 and MYB115 promotes vegetative-to-embryonic transition in *Arabidopsis*. Cell Res 19:224–235

Wuest SE, Vijverberg K, Schmidt A, Weiss M, Gheyselinck J, Lohr M, Wellmer F, Rahnenführer J, von Mering C, Grossniklaus U (2010) *Arabidopsis* female gametophyte gene expression map reveals similarities between plant and animal gametes. Curr Biol 20:506–512

Yadegari R, Drews GN (2004) Female gametophyte development. Plant Cell 16:S133–S141

Yang W, Jefferson RA, Huttner E, Moore JM, Gagliano WB, Grossniklaus U (2005) An egg apparatus-specific enhancer of *Arabidopsis*, identified by enhancer detection. Plant Physiol 139:1421–1432

Yu H-J, Hogan P, Sundaresan V (2005) Analysis of the female gametophyte transcriptome of *Arabidopsis* by comparative expression profiling. Plant Physiol 139:1853–1869

Zuo J, Niu QW, Frugis G, Chua NH (2002) The *WUSCHEL* gene promotes vegetative-to-embryonic transition in *Arabidopsis*. Plant J 30:349–359